

# The ORGANICS experiment on BIOPAN V: UV and space exposure of aromatic compounds

Pascale Ehrenfreund<sup>a,\*</sup>, Richard Ruiterkamp<sup>a</sup>, Zan Peeters<sup>a</sup>, Bernard Foing<sup>b</sup>,  
Farid Salama<sup>c</sup>, Zita Martins<sup>a</sup>

<sup>a</sup>*Astrobiology Laboratory, Leiden Institute of Chemistry, P.O. Box 9502, 2300 RA Leiden, The Netherlands*

<sup>b</sup>*ESA Research and Scientific Support Department, P.O. Box 299, 2200 AG Noordwijk, The Netherlands*

<sup>c</sup>*Space Science Division, NASA Ames Research Center, MS 245-6, Moffett Field, CA 94035, USA*

Received 3 March 2006; received in revised form 5 July 2006; accepted 6 July 2006

Available online 17 January 2007

## Abstract

We studied the stability of aromatic compounds in low Earth orbit environment and describe the scientific results and successful flight of the ORGANICS experiment on-board the BIOPAN V space exposure facility. This experiment investigated the photo stability of large organic molecules in low Earth orbit. Thin films of selected organic molecules, such as polycyclic aromatic hydrocarbons (PAHs) and the fullerene C<sub>60</sub> were subjected to the low Earth orbit environment and the samples were monitored before and after flight. PAHs and fullerenes have been proposed as carriers for a number of astronomical absorption and emission features and are also identified in meteorites. Our experiment on BIOPAN V was exposed to a total fluence of 602.45 kJ m<sup>-2</sup> for photons in the range 170–280 nm. The experiment was also intended as a hardware test-flight for a long-term exposure experiment (Survival of organics in space) on the EXPOSE facility on the International Space Station (ISS). For the small fluence that was collected during the BIOPAN V experiment we found little evidence of photo-destruction. The results confirm that PAH molecules are very stable compounds in space. The small differences in destruction rates that are expected to arise among the PAH samples as a function of molecular size and structure will only show after the longer irradiation fluences that are expected in the exposure experiment on the ISS.

© 2006 Elsevier Ltd. All rights reserved.

*Keywords:* PAHs; Interstellar molecules; Space research; Low earth orbit exposure; Biopan; International Space Station; Photo-stability

## 1. Introduction

Carbon chemistry in space occurs most efficiently in circumstellar and diffuse interstellar clouds. The circumstellar envelopes of carbon-rich evolved stars are the heart of the most complex carbon chemistry that is analogous to soot formation (Henning et al., 2004). Benzene chemistry in those regions is the first step to polycyclic aromatic hydrocarbons (PAHs), fullerene-type material and large aromatic networks (Frenklach and Feigelson, 1989; Pascoli and Polleux, 2000; Ruiterkamp et al., 2005a). All three isoforms of carbon; diamond, graphite and fullerene, are thought to be present in space environments (Cataldo,

2004). Aromatic macromolecules and PAHs are the dominant organic material in space (Henning and Salama, 1998; Ehrenfreund and Charnley, 2000; Pendleton and Allamandola, 2002; Mennella et al., 1998; Allamandola et al., 1999; Dartois et al., 2004).

Large carbon-bearing molecules, such as PAHs, fullerenes and unsaturated chains are also thought to be present in the interstellar medium (ISM) in various charge states (see Henning and Salama, 1998 and Ehrenfreund and Charnley, 2000 for reviews). PAHs are observed in galactic and extragalactic regions and are probably the most abundant carbonaceous gas phase molecules in space (Tielens et al., 1999; Yan et al., 2005). Laboratory studies and theoretical calculations have provided important insights into their size and charge state distribution (e.g. Salama et al., 1996; Allamandola et al., 1999; Ruiterkamp

\*Corresponding author. Tel.: +31 71 5274541; fax: +31 71 5274397.

E-mail address: [p.ehrenfreund@chem.leidenuniv.nl](mailto:p.ehrenfreund@chem.leidenuniv.nl) (P. Ehrenfreund).

et al., 2005b). PAHs have been identified in meteorites, interplanetary dust particles (IDPs) and in comets (see Ehrenfreund and Charnley, 2000 for a review).

In the ISM mixed neutral and ionized PAHs are thought to be responsible for the unidentified infrared emission bands (UIBs) and the UV and visible diffuse interstellar bands (DIBs) (Allamandola et al., 1999; Herbig, 1995). In UV-irradiated regions, a significant fraction of PAH molecules can be partly dehydrogenated or even fragmented (Allain et al., 1996a; Allain et al., 1996b; Vuong and Foing, 2000; Le Page et al., 2001) and the abundance of any PAH depends on its formation, destruction, ionization and hydrogenation state. We can expect that during the formation process of PAHs many isomers are formed. The physical conditions in the ISM will provide a selection mechanism that favors individual PAHs or PAH families (Ruiterkamp et al., 2005b). The famous polyhedral molecules first discussed by Kroto et al. (1985) could be important carriers of carbon in our Galaxy.  $C_{60}$  was first isolated by Krätschmer et al. (1990). Two DIBs in the near infrared have been assigned to the  $C_{60}$  cation (Foing and Ehrenfreund, 1994, 1997). In the Allende meteorite  $C_{60}$  and higher fullerenes up to  $C_{240}$  have been detected (Becker and Bunch, 1997).

In order to understand the nature and abundance of organics in space, knowledge on the survival times (or destruction rates) of these molecules is crucial. Destruction of large organic molecules in space is governed predominantly by UV photolysis and cosmic rays bombardment.

In this paper we describe the BIOPAN facility and the ORGANICS experiment package in Section 2. The pre-flight sample preparation is discussed in Section 3 and we proceed with the presentation of the results in Section 4 and conclusions in Section 5.

## 2. The BIOPAN facility

BIOPAN is a multi-user space exposure platform that is attached on the outer hull of the Russian FOTON capsule (see Fig. 1). Between 1992 and 1999 BIOPAN successfully completed three 2-week missions whereby 16 experiments were conducted in the fields of astrobiology, chemical evolution, radiation biology and radiation dosimetry (Demets et al., 2005). In 2002, the fourth flight of BIOPAN failed when the launcher exploded. FOTON missions typically spend about 2 weeks in orbit and during this time the BIOPAN module exposes its payload to the low Earth orbit (LEO) UV environment (see Fig. 2). BIOPAN is a “pan” like container that carries its payload experiments on the inner side of the two lids. After successful insertion in the final mission orbit the BIOPAN is opened by a tele-command from the ground control center. After the lid is opened the experiment packages are exposed to space conditions until a tele-command closes the lid and seals the payload for re-entry. Exposed samples are then transported under controlled conditions back to the investigator’s laboratories. FOTON-M2 and BIOPAN V were launched successfully on 31st May 2005 on board a Soyuz carrier rocket and stayed in orbit for 15.8 days. The BIOPAN module that contained 11 experiment packages was recovered after landing and the ORGANICS experiment package was shipped back to the PI laboratory (P. Ehrenfreund/Leiden University).

FOTON-M2 was launched from pad 3 of the Baikonur launch site on May 31, 2005 at 12:00 UCT and landed June 16, 2005 on a site 170 km south of Kostanaya (latitude  $51^{\circ}40'38.9''$  North, longitude  $63^{\circ}42'44.6''$  East) at 07:37 UCT. Completing a total of 253 orbits the total flight



Fig. 1. The Foton capsule and the BIOPAN module after touchdown in the Kazachstan tundra. The BIOPAN is the circular object on the right bottom side of the spherical Foton capsule.

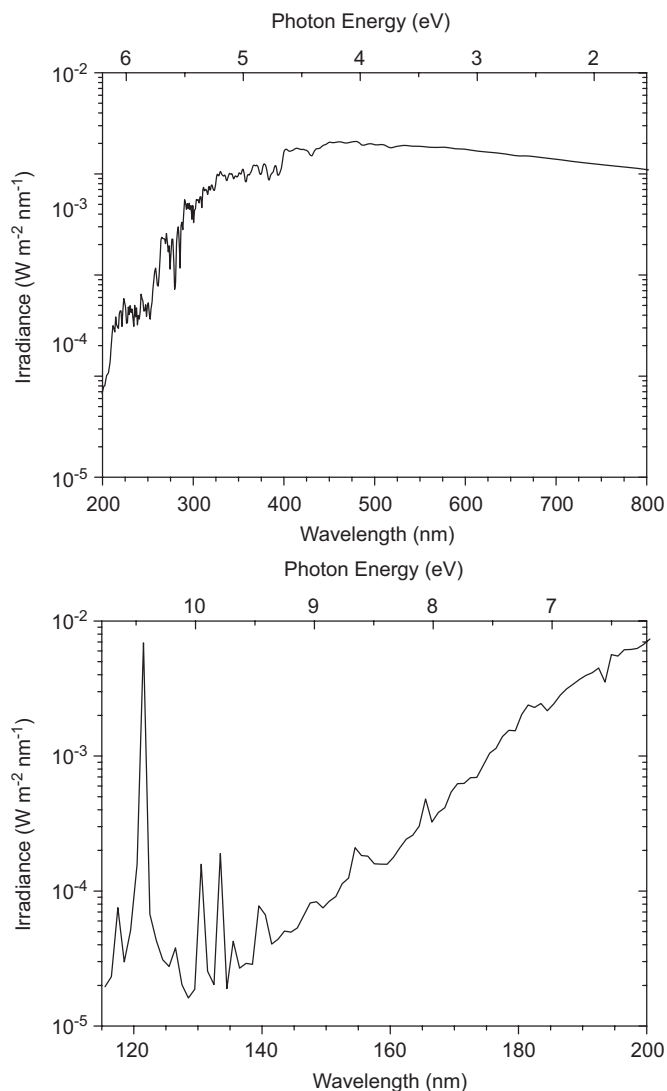


Fig. 2. Averaged solar spectral irradiance during the BIOPAN flight. The top panel shows the solar spectral irradiance for the range of the R3D sensor package. The spectrum was composed of the average of solar spectra collected during the duration of the BIOPAN flight (31 May–16 June 2005) by the SORCE satellite ([http://lasp.colorado.edu/sorce/sorce\\_data\\_access/](http://lasp.colorado.edu/sorce/sorce_data_access/)). The bottom panel shows the high-energy part of the solar spectrum down to 115 nm. The choice of window materials in the ORGANICS experiment package allows transmission of wavelengths down to 120 nm. Note that in the solar UV spectrum the Lyman- $\alpha$  irradiance (121 nm) is 250 times stronger than the directly surrounding irradiance.

duration was 379 h and 26 min (15 days 19 h 26 min = 15.8 days). The FOTON-M2 capsule was inserted into an orbit with 90 min period and 62.99° inclination. The apogee shifted from 306.4 initially to 302.1 km at the end of the mission and the perigee from 257.7 to 253.4 km. During the entire mission the temperature was recorded and is graphically displayed in Fig. 3.

Although the mission was nominal in its orbital characteristics there were some problems with the data collection of photon and particle fluxes. The on-board memory shorted out after four orbits probably due to a

heavy particle impact directly on the memory chip. No data from the primary sensor package were stored after the heavy particle impact event. All flux and dose measurements that are presented here were kindly provided by the R3D experiment team (University Erlangen-Nürnberg, Department of Plant Ecophysiology. Prof. D.-P. Häder, Dr. P. Richter, M. Schuster; Bulgarian Academy of Sciences, Dr. T. Dachev). The R3D experiment package obtained spectral information in seven spectral bands ranging from 170 to 770 nm (see Table 1 for definition of the spectral sensor bands). The irradiance and time integrated irradiance over the BIOPAN flight (fluence) per sensor is given in Table 1. Additionally the R3D package contained sensors to record the dose of ionizing radiation and observed an average daily dose of 213.36  $\mu\text{Gy day}^{-1}$ .

The sample package for the ORGANICS experiment on BIOPAN consists of eight arbitrarily selected small PAHs and the fullerene  $\text{C}_{60}$  (see Fig. 4). The goal was to test the stability of such compounds when exposed to space conditions. PAH molecules such as shown in Fig. 4 are stable and are expected to survive the harsh interstellar conditions. It was our goal to identify the most stable PAH and fullerene species to gain insights into PAH chemistry and to guide our laboratory spectroscopy program. Due to the large number of possible PAH isomers it is not feasible to obtain accurate spectra for an entire set. We have specifically selected small PAHs that contain 3, 4, 5 or 7 aromatic rings. We assume that larger PAHs are formed from smaller ones that act as precursors. Differences in photo-stability will lead to higher abundances of the more stable PAH precursor molecules during synthesis thereby leading to specific homologue series as reaction products. If, for example, 1,2-benzanthracene is more stable than 2,3-benzanthracene for UV and cosmic ray particle irradiation, it is more likely that the homologue series based on 1,2-benzanthracene (i.e. 1,2-benznaphthacene; 1,2-benzpentacene,...) will prevail over homologue series based on 2,3-benzanthracene (i.e. 2,3-benznaphthacene; 2,3-benzpentacene,...) in the ISM. We have selected all PAHs with 3 and 4 aromatic rings that are readily available and are not toxic or carcinogens. Additionally, we selected perylene and coronene as PAHs with 5 and 7 aromatic rings, respectively. The major decomposition products of small PAHs and  $\text{C}_{60}$  that are expected for those experiments are a variety of dehydrogenated PAHs,  $\text{C}_2\text{H}_2$ , H, and possibly  $\text{C}_2$  and other radicals in case of PAH skeleton destruction.

The solar spectrum at LEO can be scaled exactly to any interplanetary conditions (by correction to the inverse square of distance). Therefore, BIOPAN can obtain information directly relevant for studying the survival of interplanetary organics. However, cosmic rays and solar particle penetration is different in LEO compared to interplanetary and interstellar space. Solar UV can be simulated in the laboratory by combining a Xenon lamp (above 200 nm) and an  $\text{H}_2$  lamp (with emission

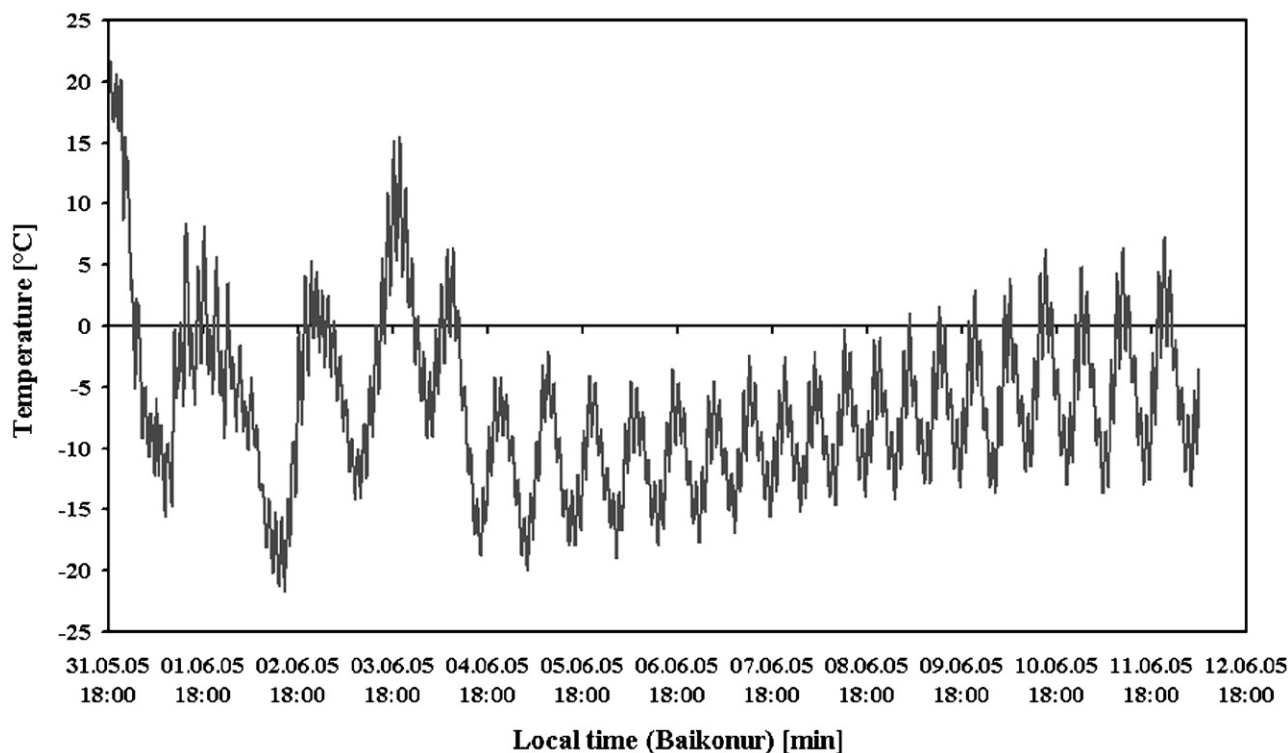


Fig. 3. Temperature profile for the ORGANICS experiment package, kindly provided by the Department of Plant Ecophysiology; University Erlangen-Nürnberg; D.P. Häder, P. Richter, M. Schuster. The maximum temperature was experienced during integration and did not exceed 20 °C. The minimum temperature was obtained just after opening of the BIOPAN lid and did not drop below –22.5 °C.

Table 1  
Irradiance and fluence at the sample level of the BIOPAN V mission

Area	Wavelengths (nm)	Irradiance ( $\text{W m}^{-2}$ )	Fluence ( $\text{kJ m}^{-2}$ )
UV-C I	170–280	6.1228	602.45
UV-C II	200–280	6.0333	629.04
UV-C III	215–280	5.7691	638.71
UV-B	280–315	26.8294	4721.53
UV-A	315–400	226.6663	49300
Vis I	400–700	439.5055	97790
Vis II	400–770	469.0552	91920

Data were collected in seven spectral bands ranging from 170 to 770 nm (data were kindly provided by the R3D experiment team).

at 120 and 160 nm, simulating solar Lyman  $\alpha$  and vacuum UV emission). However the operational lifetime of such a laboratory simulation is limited in practice to 24 h. Above 24 h vacuum and radiation conditions are not anymore reliable due to background water accretion and small in-leaks that lead to compounds such as OH radicals that influence the destruction rate of organic molecules. Furthermore, the formation of color centers in UV transparent windows reduces the UV flux after a few hours of irradiation. For processes relevant to the energy range at 7 eV, space exposure experiments such as BIOPAN (380 h, with 15% effective solar pointing) can simulate 600 years diffuse interstellar radiation field and future solar pointing facilities may achieve more.

The objectives of the ORGANICS experiment on BIOPAN are: (i) to study the photo-stability of selected PAH and fullerene-type molecules in interplanetary environment to allow a comparison with space data and, in particular, with the spectra of DIBs; (ii) to identify promising target molecules for further space exposure studies; (iii) to allow an estimation of dissociation regimes for organic molecules in different space environments (interstellar, interplanetary, Earth atmosphere, etc.) and (iv) as test flight for EXPOSE.

### 3. Materials and methods

PAHs and fullerenes were deposited onto  $\text{MgF}_2$  substrate windows (thickness = 1 mm, radius = 7 mm) by heating a PAH-loaded furnace under vacuum. The deposition chamber had a diameter of 30 cm and was evacuated to a pressure of  $1 \times 10^{-5}$  mbar by a rotary vane roughing pump (SaveVac 140) and molecular turbo pump unit (Pfeiffer Vacuum D35614 Asslar). Substrate windows were positioned directly above the sublimation furnace at a distance of 20 cm. The furnace was heated by a 5  $\Omega$  resistor (Arcol HS10) and the temperature was monitored by a PT100 temperature sensor. The sublimation temperature could be set to temperatures up to 360 °C. During vacuum deposition the sublimed PAH sample coated the  $\text{MgF}_2$  sample windows. The sample thickness was monitored by observing the interference fringes in a laser signal (670 nm)

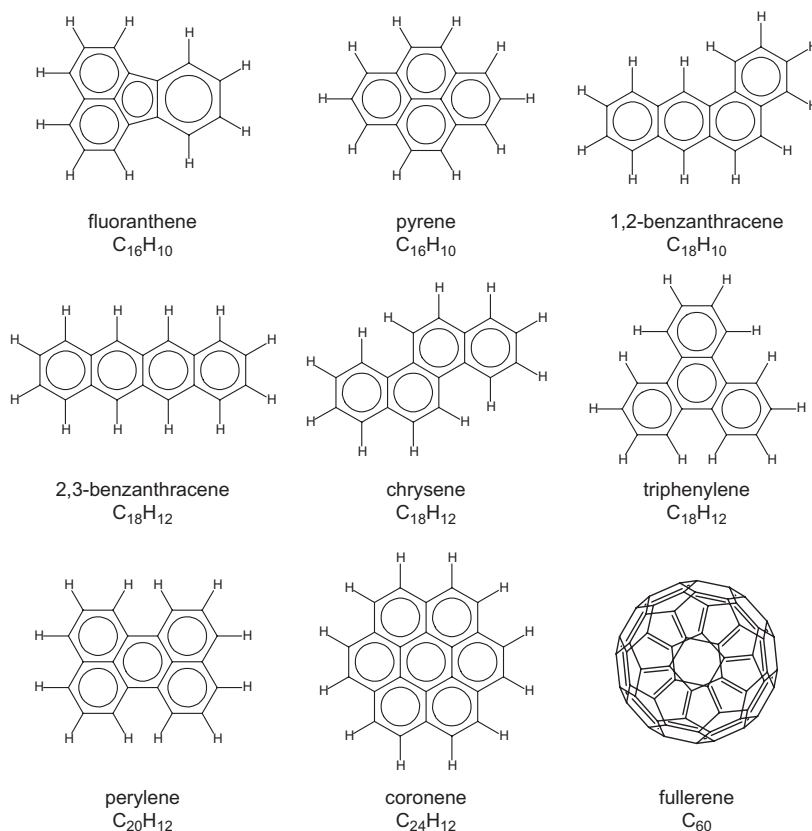


Fig. 4. Polycyclic aromatic hydrocarbons (PAHs) and fullerene  $C_{60}$  that were selected for the ORGANICS experiments. The PAH samples contain 4, 5 or 7 aromatic units.

that was reflected off the sample surface. Using this method we were able to create thin ( $< 1 \mu\text{m}$ ) films of the PAH sample material. PAH samples were selected based on availability and molecular size and include fluoranthene ( $C_{16}H_{10}$ , Aldrich 99%), pyrene ( $C_{16}H_{10}$ , Aldrich sublimed 99%), 1,2-benzanthracene ( $C_{18}H_{12}$ , Aldrich 99%), 2,3-benzanthracene ( $C_{18}H_{12}$ , Aldrich 98%), chrysene ( $C_{18}H_{12}$ , Aldrich zone-refined 98%), triphenylene ( $C_{18}H_{12}$ , Aldrich 98%), perylene ( $C_{20}H_{12}$ , Aldrich 99%), coronene ( $C_{24}H_{12}$ , Aldrich sublimed 99%), and fullerene  $C_{60}$  (SES Research 99,9+%). After deposition, the film thickness was recorded a second time using atomic force microscopy (AFM, Digital instruments, multimode scanning probe microscope) in contact mode (see Fig. 5 for a typical film surface). This was performed by scratching the film to uncover the substrate level and measuring the thickness across the scratch. Typical film thicknesses were 100–600 nm. Before and after exposure to space conditions infrared (IR) spectra, using a Biorad Excalibur FTS 4000 and UV/Vis spectra (Varian Carry UV), were recorded.

The experimental hardware used in the ORGANICS experiment on BIOPAN is depicted in Figs. 6 and 7. Samples were contained in aluminum hexagonal sample cells that are closed by two 1 mm thick  $MgF_2$  windows that allow transmission down to 120 nm. These windows are separated by a Viton O-ring and kept in place by a delrin fitting ring which is itself fitted with a viton O-ring to keep

it in place (see Fig. 5). This allows us to perform in situ spectroscopy through the closed sample cell without opening the cells (*Note:  $MgF_2$  cuts off transmission in the IR region of the electromagnetic spectrum at  $1000 \text{ cm}^{-1}$* ). The sample cells are contained in aluminum sample containers that are closed by stainless-steel bolts (M3). All aluminum surfaces were treated with Alodine 1200S to ensure electrical conductivity, in order to prevent discharges during flight. Samples were deposited as thin (0.3–0.6  $\mu\text{m}$ ) solid films on the  $MgF_2$  window, facing zenith. All samples were closed in a sealed glove-box and stored under  $\sim 1$  atm argon. All samples were accompanied by unexposed counterparts that were positioned just underneath the sample trays exposed to solar photons. The bottom and top samples are separated by a thin aluminum sheet that blocks all UV and visible solar photons. This configuration allows only passage of energetic particles to the bottom samples. The sample holder is fixed on a base-plate that is mounted on the BIOPAN experiment plate (see Fig. 7).

The experimental parameters that are compatible with the experimental setup and choice of materials ensured the passage of photons with a wavelength between 120 and 1000 nm, and provided a shielding of  $1 \text{ g cm}^{-2}$  above the deepest nested samples. The solar electrons and protons with energies between 5 and 40 MeV/nuc are almost fully absorbed by the shielding density of the first  $MgF_2$

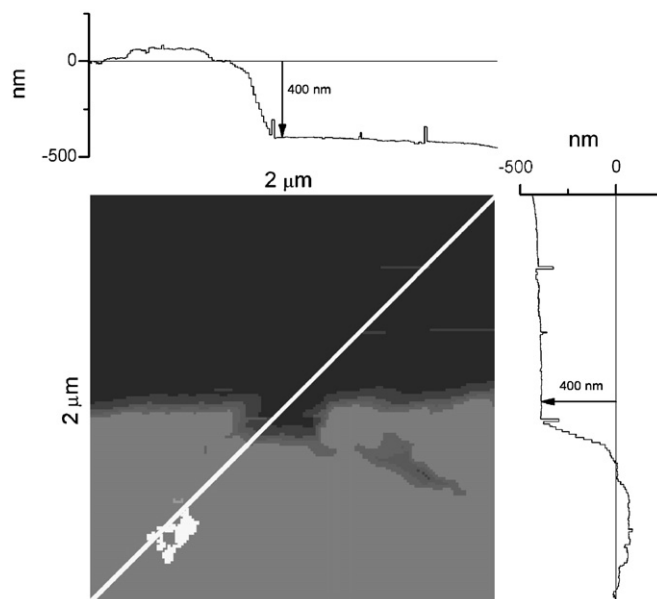


Fig. 5. Continuous mode AFM image of a  $\sim 400$  nm layer of perylene on an  $\text{MgF}_2$  substrate. The layer thickness (indicated by color coding) was measured by removing the sample layer with a needle to uncover the substrate level. The height in nm for the cross section along the white line is indicated in the top and right panels. Profile and layer thickness are similar for all used PAH films. Exceptions are discussed in Section 4. The elevation in the lower left hand corner of the image is debris scraped out of the scratch.

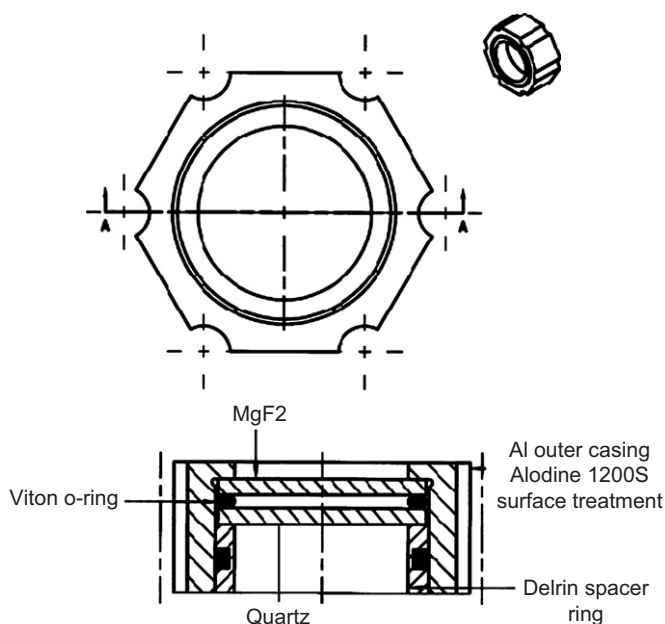


Fig. 6. Schematic view of the ORGANICS sample cells (on BIOPAN). Two layers of sample cells (illuminated and dark control) are packed together inside a container separated by a sheet of aluminum foil. Each sample cell contains (from illuminated to dark side) a  $\text{MgF}_2$  window that contains the deposited molecules, a Viton O-ring to close the sample compartment, a quartz window as bottom sealing window and a Delrin spacer with O-ring as fixture.

window. The high-energy (10–1000 MeV/nuc) particles will penetrate all samples. Since the high-energy particle flux is very small we can effectively consider the bottom samples as dark control (i.e. not exposed to the solar UV radiation).

Laboratory simulations discussed in the result section and Fig. 17 were performed in a high-vacuum set-up as described by Peeters et al. (2003) with a background pressure of  $\sim 10^{-9}$  mbar. The BIOPAN sample cells were suspended in this chamber and irradiated using a microwave excited hydrogen flow UV lamp (Ophos) with a flux of  $4.6 \times 10^{14}$  photons  $\text{cm}^{-2} \text{s}^{-1}$ . We have exposed our PAH samples to UV radiation that is commonly used for interstellar/interplanetary simulation studies (Cottin et al., 2003) for a duration of 3 h. IR spectra were recorded in the range  $4000\text{--}500$   $\text{cm}^{-1}$  using an Excalibur FTS-4000 Fourier-transform IR spectrometer (Biorad) at  $1 \text{ cm}^{-1}$  resolution.

#### 4. Results

Although no sensors were available to measure the absorbed solar irradiance below 170 nm we were able to deduce the fluence for the BIOPAN flight from solar spectra. We have used spectra that were recorded by the SORCE satellite during the FOTON-M2 mission (see [http://lasp.colorado.edu/sorce/sorce\\_data\\_access/](http://lasp.colorado.edu/sorce/sorce_data_access/)). We show the averaged spectrum over the 16 days of the experiment in Fig. 2. Since the samples were coated onto  $\text{MgF}_2$  windows and the ionization energies of our PAH samples are in the order of 7 eV we are more interested in the spectral range between 120 and 170 nm. The equivalent duration of solar exposure was 58.8 h. Note also that the 121 nm Lyman- $\alpha$  irradiance is some 250 times stronger than the directly surrounding irradiance. When we extrapolate the observed fluence from the R3D experiment package (that only collected in the range 170–770 nm) to

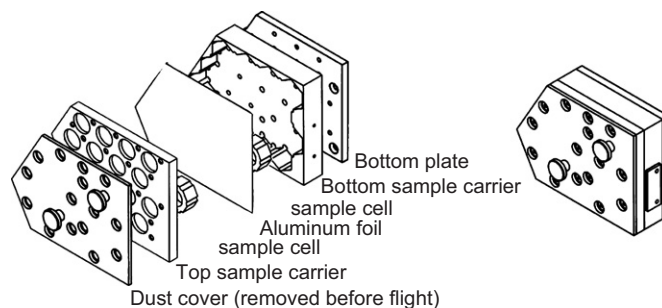


Fig. 7. Configuration of the ORGANICS sample package on BIOPAN. Two layers of sample cells (illuminated and dark control) are packed together inside a container separated by a thin aluminum foil. The top of the container is covered with a dark dust plate that is removed before flight. The package is fixed on an interface plate (that is mounted to the BIOPAN bottom plate).

the high-energy part of the solar spectrum we obtain a fluence of  $1.367 \text{ [kJ m}^{-2}]$  for the 120–170 nm range (resembling our laboratory UV lamp) and  $0.724 \text{ [kJ m}^{-2}]$  for the Lyman- $\alpha$  range.

Samples were measured before and after flight in order to examine the effects of space exposure. Additionally, ground and dark control experiments allowed to compare the effects of particle irradiation and UV irradiation, combined and separately. Pre- and post-flight analysis comprised in situ (without opening the sample cells) UV/Vis and IR spectroscopic measurements. The purity of the samples was determined by high performance liquid chromatography (HPLC) prior to deposition and after deposition to account for any contamination during vacuum deposition. Samples were dissolved from the  $\text{MgF}_2$  disks in  $500 \mu\text{l}$  acetonitrile ( $\text{CH}_3\text{CN}$ , HPLC grade). No contamination was detected and we conclude that our deposition technique was sufficiently clean. In order to use chromatographic methods (such as liquid chromatography) or mass spectrometry to measure accurate destruction rates the material needs to be dissolved from the  $\text{MgF}_2$  disks. The very small destruction rates achieved in these experiments (less than 1% for most PAHs) are comparable to the loss of material during the transfer process. Therefore we have concentrated on UV/Vis and IR spectroscopic measurements that give the most accurate results and diagnostic.

In Figs. 8 through 16 we show the UV/Visible and IR spectra of PAH samples containing 1,2-benzanthracene, 2,3-benzanthracene, chrysene, coronene, fluoranthene, perylene, pyrene, triphenylene and fullerene  $\text{C}_{60}$ , respectively. In each figure the UV/Visible spectrum is shown in the top graph and the IR spectrum in the bottom graph. In each graph panel (a) depicts the spectra of a film exposed to solar UV photons on-board BIOPAN V. Panel (b) depicts the residual spectra obtained by subtraction. The solid line shows the residual spectrum after subtraction of the spectra of the dark control (sample exposed to cosmic rays on BIOPAN V but shielded from solar UV) from the spectrum of the UV-exposed sample. The dashed line shows the residual spectrum after subtraction of the control experiment

(sample that was not exposed to space conditions but stored in 1 atm in the laboratory) from the dark control sample. The residual spectra show the effects of UV photolysis (solid line) and possible destruction due to heavy particles (dashed line). Note that due to instrumental/measurement problems with the UV-exposed samples of fluoranthene, pyrene and triphenylene we show in Figs. 12, 14 and 15 in (a) the UV/Visible spectrum for the dark control (sample exposed to cosmic rays on BIOPAN V but shielded from solar UV) and in (b) the residual spectrum after subtraction of the control experiment (that was not exposed to space conditions but stored in 1 atm in the laboratory) from the dark control sample (dashed line).

#### 4.1. 1,2-benzanthracene

We present the UV/Visible and IR spectra of 1,2-benzanthracene films in Fig. 8. The spectrum of the UV-exposed sample is shown in the top panel of each graph. We note that there are absorption bands centered around 225, 265, 375 and 395 nm in the UV/Visible spectra of these samples. In the IR spectra (bottom panel) we find absorption bands around  $1240$ ,  $1277$  and  $1339 \text{ cm}^{-1}$  in the C–C aromatic stretching and C–H bending region. The C–H aromatic stretching region shows bands at  $3003$ ,  $3030$  and  $3048 \text{ cm}^{-1}$  (data not shown). The UV/Visible residual spectra that were obtained by subtraction show a possible small loss of absorption after space exposure (solid line). However, we also find a small difference between the dark control sample and the laboratory control sample (dashed line). The excess loss of absorption between the residual spectra gives an upper limit of 0.4% for the effects of UV exposure. The IR residual spectrum of the UV-exposed samples (solid line) shows small changes around the  $1400$ – $1200 \text{ cm}^{-1}$  region that could indicate photodestruction within the upper limit of 0.4%. The dashed line indicates that there is no loss of absorption between the dark control and laboratory control samples. AFM images of the samples show that the film thickness is around 700 nm, with smaller grain like patches that stick out about 100 nm from the surface.

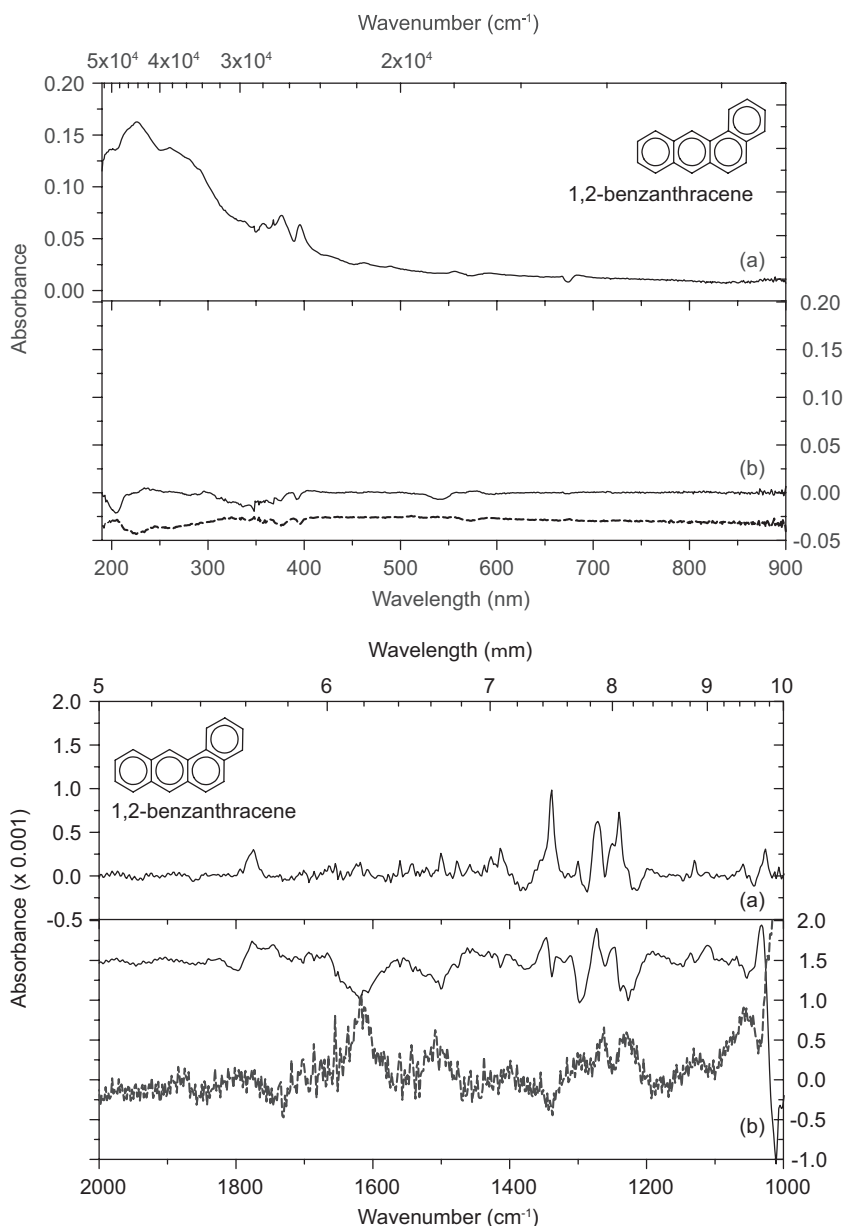


Fig. 8. Top graph shows the UV/Vis spectrum (200–900 nm) of a 1,2-benzanthracene film ( $\sim 700$  nm) deposited on a  $\text{MgF}_2$  disk while the bottom graph shows the IR spectrum (5–10  $\mu\text{m}$ ) of the same sample. In each graph panel (a) depicts the spectra of a film exposed to solar UV photons on-board BIOPAN V (except for Figs. 12, 14 and 15). Panel (b) depicts the residual spectra obtained by subtraction. The solid line shows the residual spectrum after subtraction of the spectra of the dark control (sample exposed to cosmic rays on BIOPAN V but shielded from solar UV) from the spectrum of the UV-exposed sample. The dashed line shows the residual spectrum after subtraction of the control experiment (that was not exposed to space conditions but stored under 1 atm) from the dark control sample. The residual spectra show the effects of UV photolysis (solid line) and possible destruction due to heavy particles (dashed line).

#### 4.2. 2,3-benzanthracene

The spectrum of the UV-exposed sample of 2,3-benzanthracene (panel (a) in top graph of Fig. 9) shows main absorption bands around 206, 219 and 231 nm with a broad shoulder at 273. Additionally, we also observe three bands around 440, 472 and 511 nm that are not seen in spectra of 2,3-benzanthracene dissolved in acetonitrile. These additional bands may be due to the presence of an impurity in the sample and/or to solid matrix effects. The IR spectrum

in the bottom graph in Fig. 9 shows absorption bands around 1295, 1387 and  $1462\text{cm}^{-1}$  in the C–C aromatic stretching and C–H bending region and around 3021 and  $3046\text{cm}^{-1}$  in the C–H stretching region (data not shown). Based on the UV/Visible residual spectra (top graph of Fig. 9, panel b) we conclude that there is no evidence for photodissociation since both the solid and dashed spectra indicate changes of the same (small) magnitude. The band around  $1281\text{cm}^{-1}$  in the IR residual spectrum for the UV-exposed sample (solid line) is due to a small shift in the

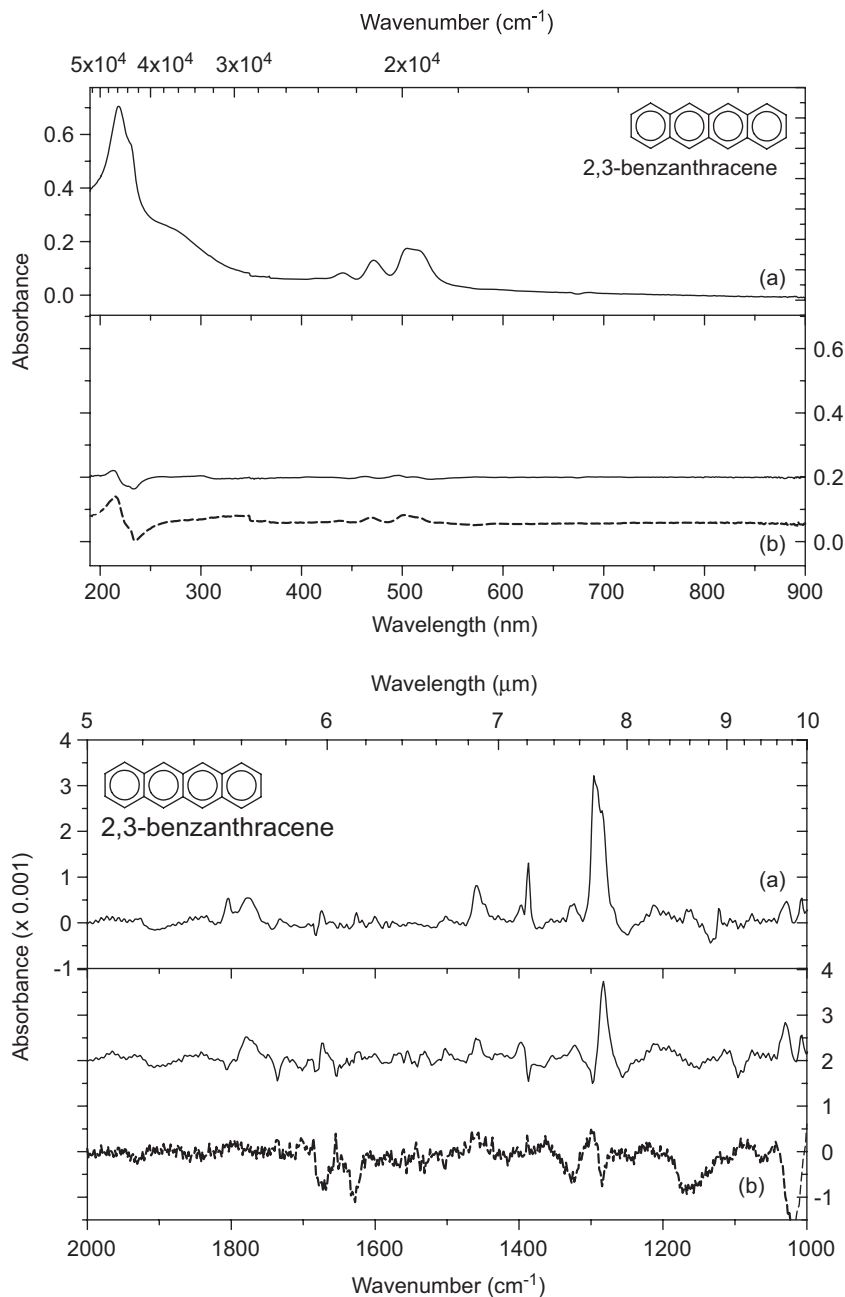


Fig. 9. Top graph shows the UV/Vis spectrum of a 2,3-benzanthracene film ( $\sim 100$  nm) deposited on a  $\text{MgF}_2$  disk while the bottom graph shows the IR spectrum of the same sample. See the figure caption of Fig. 8 for an explanation of the graph contents.

$1295\text{ cm}^{-1}$  band and is not detected in the dark control sample (dashed line). We conclude that neither from the IR residual spectra nor from the UV/Visible residual spectra we can derive an upper limit for photodissociation. An AFM image of the film showed crystals that were  $0.1\text{--}0.4\ \mu\text{m}$  in diameter and protruded up to  $1.5\ \mu\text{m}$  above the surface. Thickness has been estimated to be  $100\ \text{nm}$ .

#### 4.3. Chrysene

The top graph in Fig. 10 shows the UV/Visible spectrum of an irradiated thin film of chrysene. We find bands

around  $201$ ,  $246$ ,  $272$ ,  $304$ ,  $317$ ,  $333$ ,  $348$  and  $366\ \text{nm}$ . The IR spectrum in the bottom graph in Fig. 10 shows absorption bands around  $1192$ ,  $1246$ ,  $1263$ ,  $1300$ ,  $1433$ ,  $1487$  and  $1593\ \text{cm}^{-1}$  in the C–C aromatic stretching and C–H bending region and around  $3009$ ,  $3051$ ,  $3082$  and  $3094\ \text{cm}^{-1}$  in the aromatic C–H stretching region (data not shown). The UV/Visible and IR residual spectra shown in the bottom panels (b) indicate that no destruction or changes in the film structure have occurred during exposure to space conditions. When we determine an upper limit for destruction using the UV/Visible residual spectra we obtain less than  $0.5\%$  of the initial absorbance.

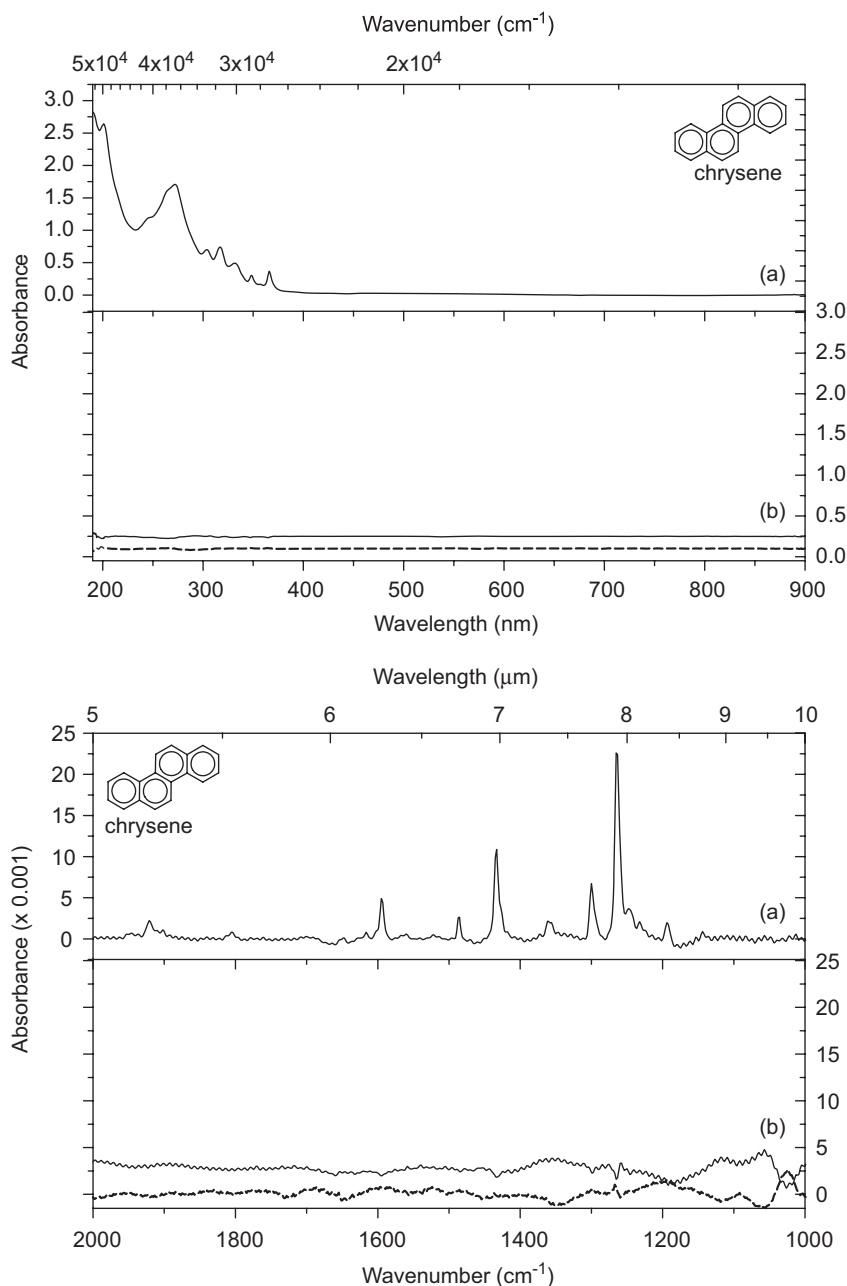


Fig. 10. Top graph shows the UV/Vis spectrum of a chrysene film ( $\sim 300$  nm) deposited on a  $\text{MgF}_2$  disk while the bottom graph shows the IR spectrum of the same sample. See the figure caption of Fig. 8 for an explanation of the graph contents.

Indeed, we also find no evidence for photodestruction from the IR residual spectra (bottom graph in Fig. 10). The film thickness of the chrysene films was 300 nm and appeared as a smooth surface without crystal structures.

#### 4.4. Coronene

The UV/Visible spectrum of an UV-exposed coronene sample is shown panel (a) of the upper graph in Fig. 11. We find two broadband systems centered around 199 and 320 nm. In the IR spectrum shown in panel (a) of the bottom graph in Fig. 11 we find absorption bands around 1136, 1310, 1501 and  $1609\text{ cm}^{-1}$  in the C–C aromatic

stretching and C–H bending region and around 3019 and  $3053\text{ cm}^{-1}$  in the aromatic C–H stretching region (data not shown). Based on the UV/Visible residual spectra in the top graph (panel b) we measure an upper limit of 0.8% loss of absorption for the UV-exposed sample (solid line). The AFM image of the coronene film showed a thin 300 nm layer of needle-like crystals covering the surface.

#### 4.5. Fluoranthene

The UV/Visible and IR spectra for fluoranthene samples are shown in Fig. 12. We observed absorption bands

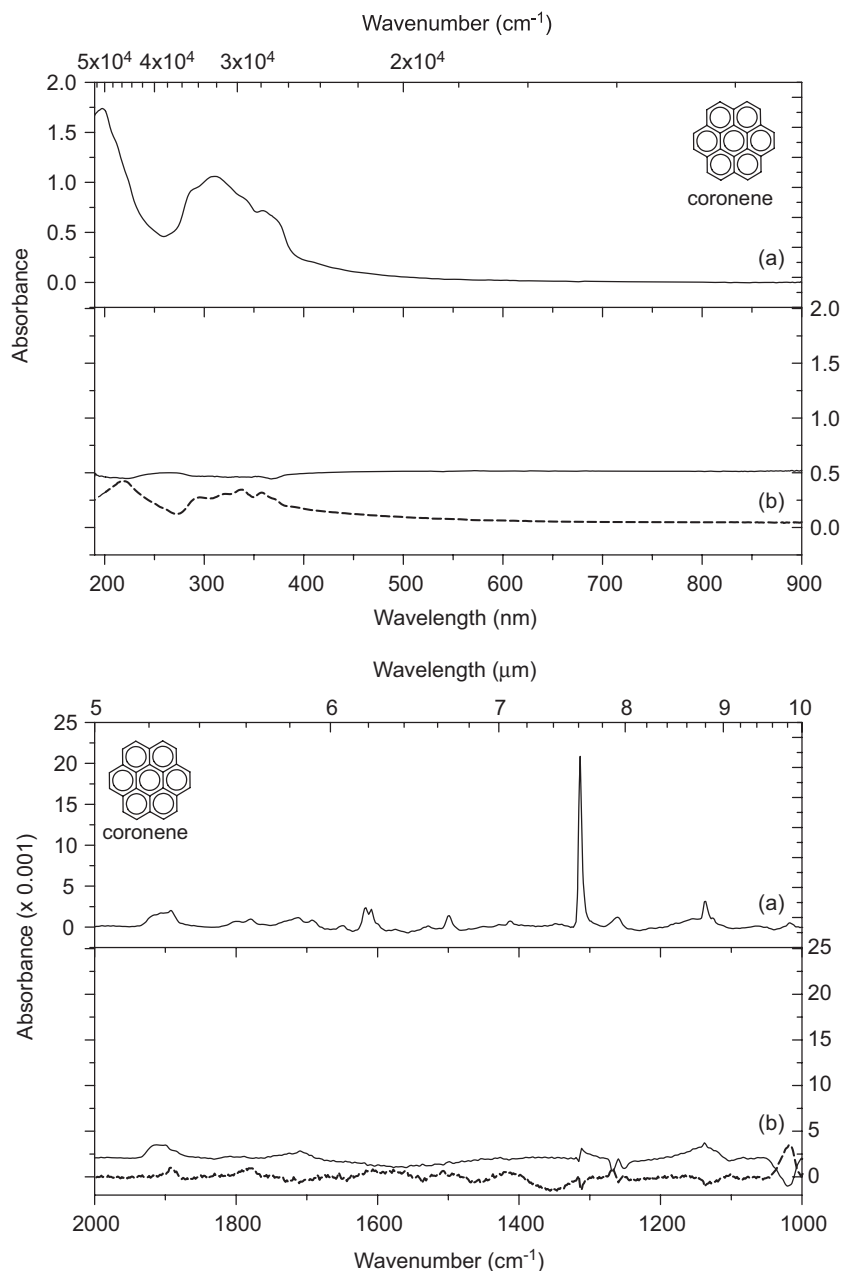


Fig. 11. Top graph shows the UV/Vis spectrum of a coronene film ( $\sim 300$  nm) deposited on MgF<sub>2</sub> disks while the bottom graph shows the IR spectrum of the same sample. See the figure caption of Fig. 8 for an explanation of the graph contents.

around 246, 313, 330 and 372 nm. Due to instrumental/measurement problems with the UV-exposed samples of fluoranthene we only show the UV/Visible spectrum for the dark control (exposed to cosmic rays on BIOPAN V but shielded from solar UV) and base our conclusions on the IR spectra alone. The IR spectrum of the UV-exposed sample in the bottom graph of Fig. 12 shows absorption bands around 1136, 1159, 1184, 1202, 1217, 1229, 1271 and 1292 cm<sup>-1</sup> in the C–H bending region, at 1368, 1412, 1427, 1439, 1451, 1474 and 1487 cm<sup>-1</sup> in the aromatic C–C stretching region and at 3036 cm<sup>-1</sup> in the aromatic C–H stretching region of the spectrum (data not shown).

The residual spectra in panel (b) in the bottom graph indicate an upper limit for destruction upon UV exposure of 0.5%. AFM images of fluoranthene films show small (1–2 μm) orthorhombic crystals and a thickness of 500 nm.

#### 4.6. Perylene

Fig. 13 shows the UV/Visible spectrum of a perylene thin film (panel (a) in the top graph) after exposure to UV radiation. We observe two broadband structures around 200 and 256 nm in the UV/Visible spectrum. The IR

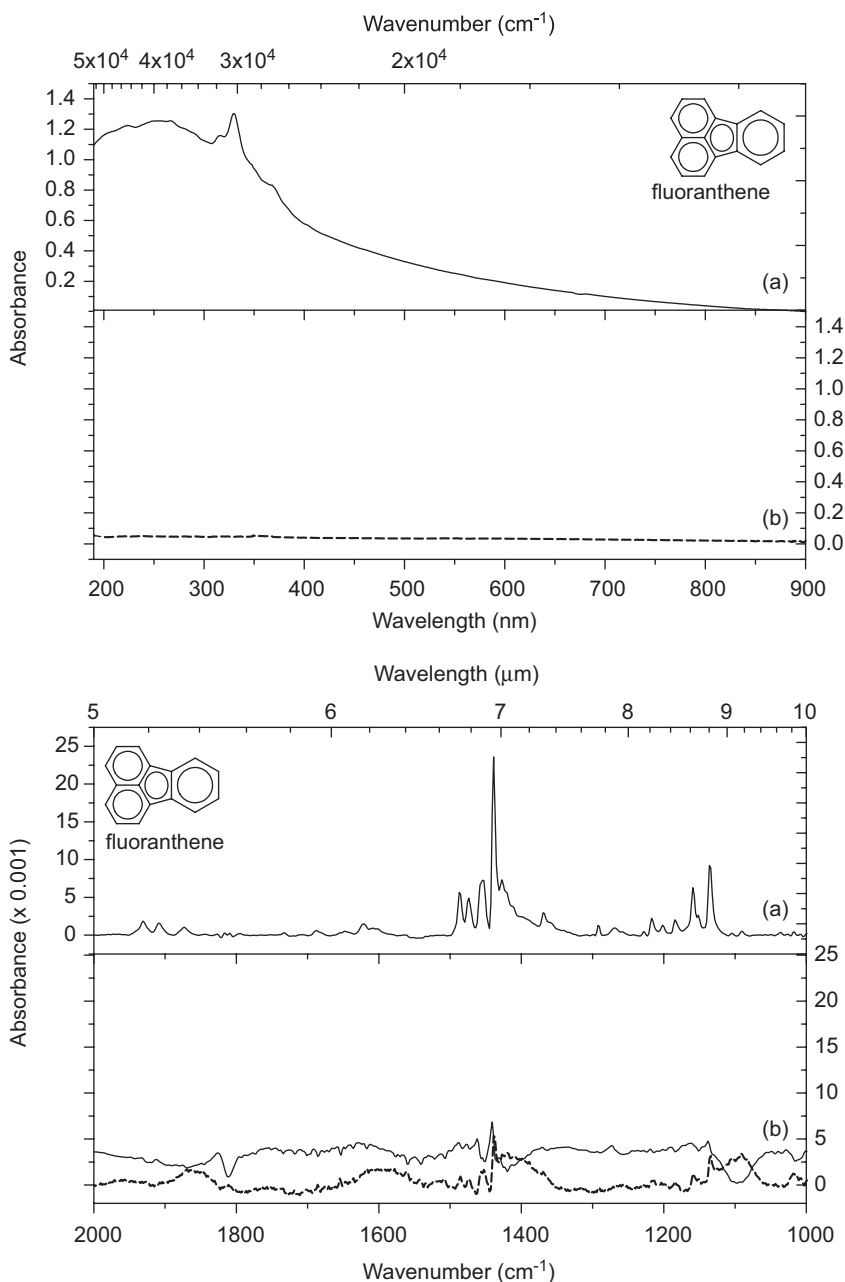


Fig. 12. Top graph shows the UV/Vis spectrum of an unexposed fluoranthene film ( $\sim 500$  nm). Due to instrumental/measurement problems with the UV-exposed samples we show in (a) the UV/Visible spectrum for the dark control (sample exposed to cosmic rays on BIOPAN V but shielded from solar UV) and in (b) the residual spectrum after subtraction of the control experiment (that was not exposed to space conditions but stored in 1 atm in the laboratory) from the dark control sample (dashed line). The bottom graph shows the IR spectrum of the exposed sample. See the figure caption of Fig. 8 and text for an explanation of the IR graph contents.

spectra of the perylene film show absorption bands around 1089, 1126, 1184, 1209, 1240, 1281, 1288 and  $1324\text{ cm}^{-1}$  in the aromatic C–H bending and around 1495, 1508,  $1605\text{ cm}^{-1}$  in the aromatic C–C stretching and overtone region. Bands at 3034 and  $3050\text{ cm}^{-1}$  appear in the aromatic C–H bending region (data not shown). Based on the residual spectra after subtraction we derive an upper limit for photodestruction upon UV exposure of less than 1%. AFM image of the perylene film showed a 400 nm thick smooth film surface.

#### 4.7. Pyrene

The UV/Visible spectrum of a pyrene film is shown in the top graph of Fig. 14. We observe absorption bands around 229, 296, 340 and 370 nm in the UV/Visible spectrum (top graph, panel a). Due to instrumental/measurement problems with the UV-exposed samples of pyrene we only show the UV/Visible spectrum for the dark control (exposed to cosmic rays on BIOPAN V but shielded from solar UV) and base our conclusions on the IR spectra

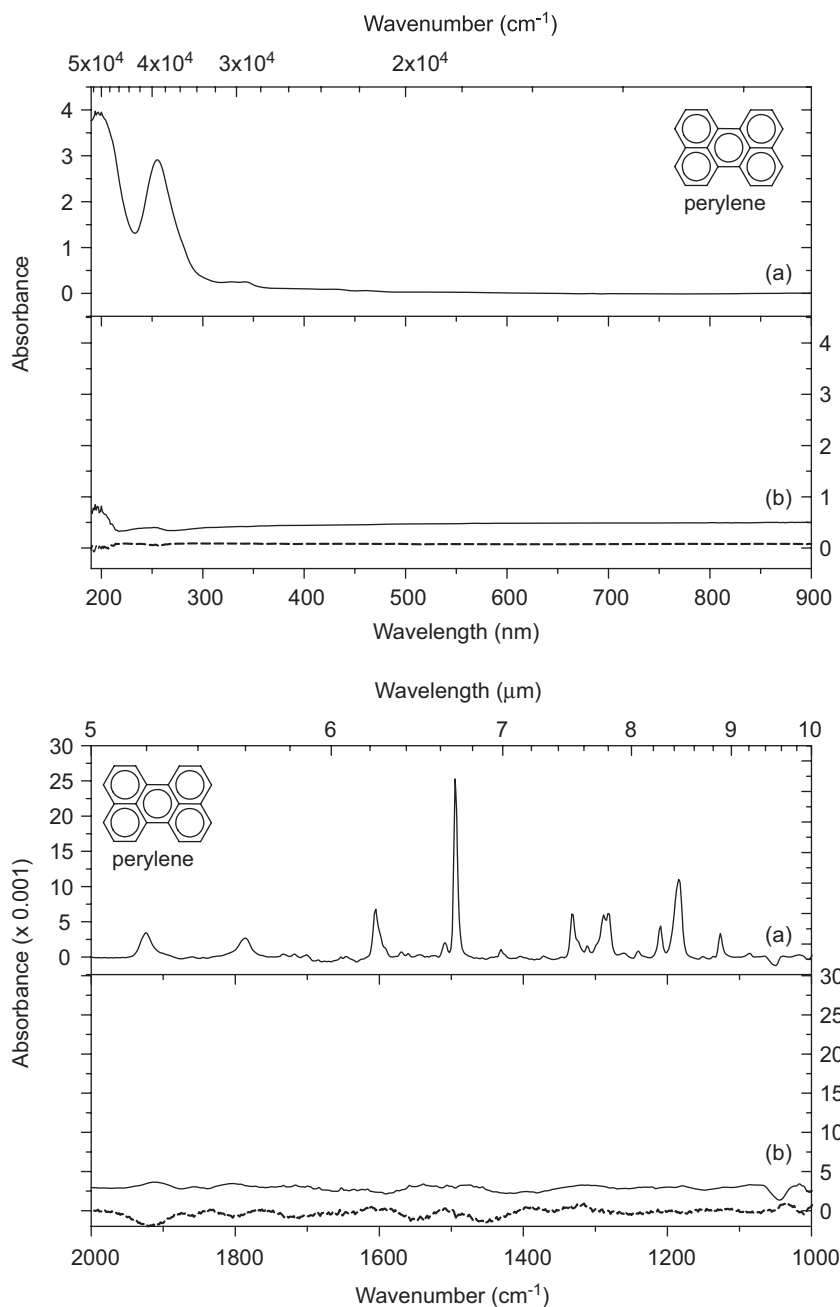


Fig. 13. Top graph shows the UV/Vis spectrum of a perylene film ( $\sim 400$  nm) deposited on a  $\text{MgF}_2$  disk while the bottom graph shows the IR spectrum of the same sample. See the figure caption of Fig. 8 for an explanation of the graph contents.

alone. IR absorption bands (bottom graph, panel a) were observed for the UV-exposed sample around 1184, 1240 and 1312  $\text{cm}^{-1}$  in the aromatic C–H bending region, at 1433, 1449, 1464, 1483 and 1595  $\text{cm}^{-1}$  in the aromatic C–C stretching region and at 3028 and 3048  $\text{cm}^{-1}$  in the aromatic C–H stretching region (data not shown). Based on the IR residual spectra (panel b, bottom graph) we obtain an upper limit for photodestruction of 0.7%. AFM images of the film compared to the same sample after deposition show the formation of orthorhombic crystals

(5–10  $\mu\text{m}$  in diameter and 0.8  $\mu\text{m}$  above the surface) and a thickness of 800 nm.

#### 4.8. Triphenylene

The UV/Visible spectrum of a triphenylene film is shown in the top graph of Fig. 15. We observe UV/Visible absorption bands around 205, 277 and 301 nm. Due to instrumental/measurement problems with the UV-exposed samples of triphenylene we only show the UV/Visible

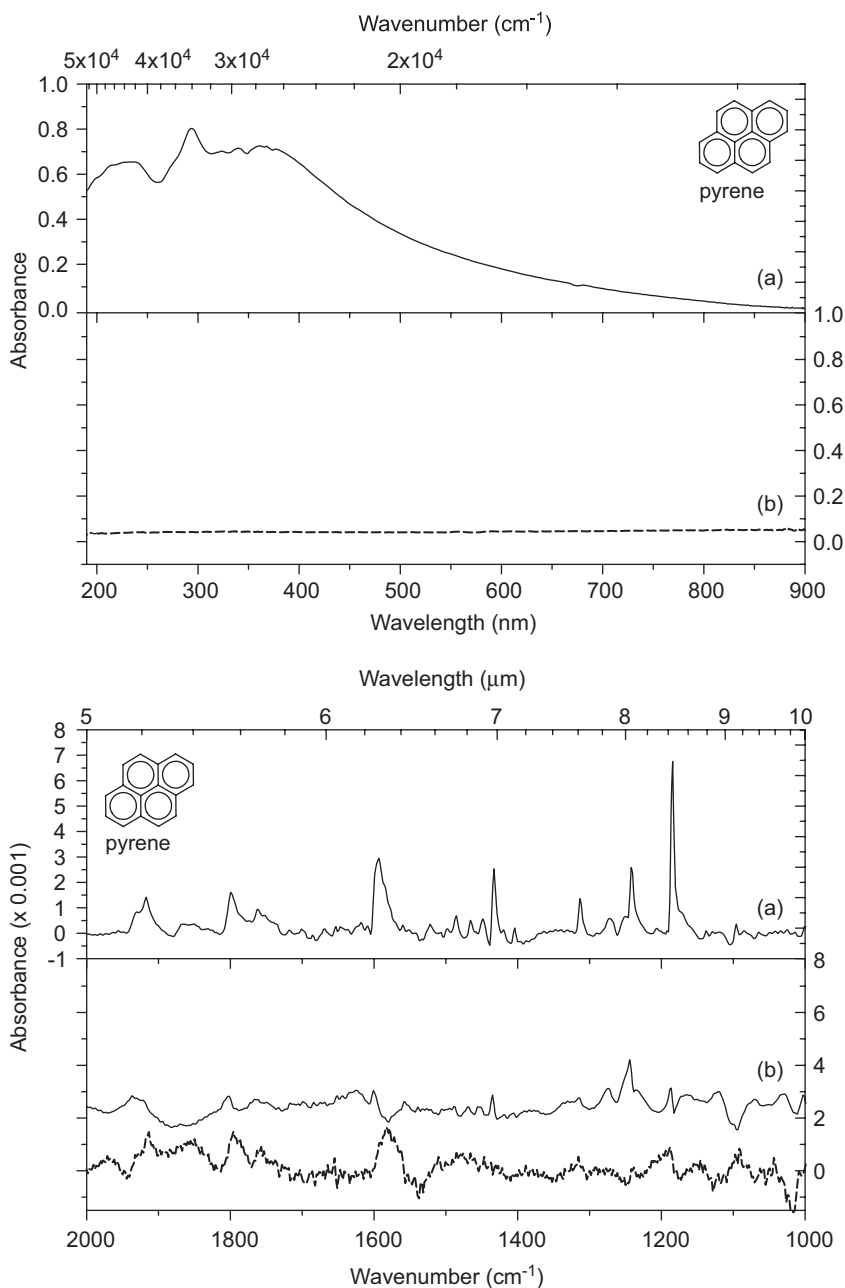


Fig. 14. Top graph shows the UV/Vis spectrum of an unexposed pyrene film ( $\sim 800$  nm) deposited on a  $\text{MgF}_2$  disk. Due to instrumental/measurement problems with the UV-exposed samples we show in (a) the UV/Visible spectrum for the dark control (sample exposed to cosmic rays on BIOPAN V but shielded from solar UV) and in (b) the residual spectrum after subtraction of the control experiment (that was not exposed to space conditions but stored in 1 atm in the laboratory) from the dark control sample (dashed line). The bottom graph shows the IR spectrum of the exposed sample. See the caption of Fig. 8 and text for an explanation of the IR graph contents.

spectrum for the dark control (exposed to cosmic rays on BIOPAN V but shielded from solar UV) and base our conclusions on the IR spectra alone. The IR spectrum of the UV-exposed triphenylene films (bottom graph) shows absorption bands around 1244, 1433 and 1496  $\text{cm}^{-1}$  in the C–H bending and C–H stretching region and a weak band around 3067  $\text{cm}^{-1}$  in the aromatic C–H stretching region (data not shown). From the IR residual spectra we obtained an upper limit of 0.3% destruction upon UV exposure. AFM images of the triphenylene film showed

elongated needle-like structures that are  $\sim 10$  nm in length and 1–2  $\mu\text{m}$  in diameter. The thickness was estimated to be 500 nm.

#### 4.9. Fullerene $\text{C}_{60}$

A UV/Visible spectrum of a fullerene  $\text{C}_{60}$  film is shown in Fig. 16. We observe no band systems in the UV/Visible apart from a broadband system centered around 200 nm. Since the film thickness was very thin ( $< 100$  nm) we could

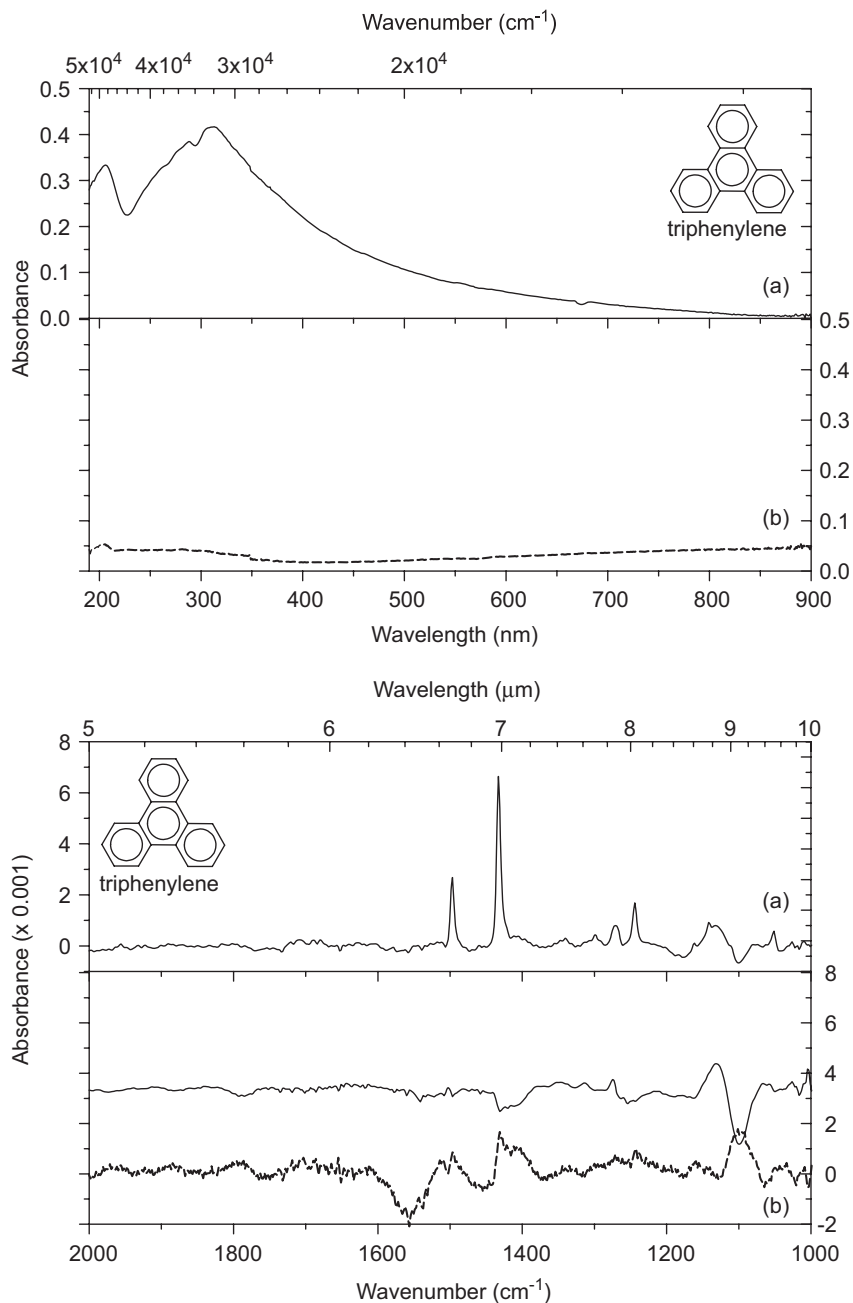


Fig. 15. Top graph shows the UV/Vis spectrum of an unexposed triphenylene film ( $\sim 500$  nm) deposited on a  $\text{MgF}_2$  disk. Due to instrumental/measurement problems with the UV-exposed samples we show in (a) the UV/Visible spectrum for the dark control (sample exposed to cosmic rays on BIOPAN V but shielded from solar UV) and in (b) the residual spectrum after subtraction of the control experiment (that was not exposed to space conditions but stored in 1 Atm in the laboratory) from the dark control sample (dashed line). The bottom graph shows the IR spectrum of the exposed sample. See the caption of Fig. 8 and text for an explanation of the IR graph contents.

not obtain a meaningful IR spectrum. The residual spectra in panels (b) indicate an upper limit of 0.7% for the photodestruction upon UV exposure.

#### 4.10. Laboratory simulation studies

We have also performed laboratory simulation studies for a number of PAHs exposed on BIOPAN V. The BIOPAN sample cells were suspended in a high vacuum

chamber and irradiated with a hydrogen flow UV lamp (Peeters et al., 2003).  $\text{MgF}_2$  sample windows transmit photons with wavelengths longer than 120 nm. We have exposed our PAH samples to UV radiation that is commonly used for interstellar/interplanetary simulation studies (Cottin et al., 2003) for a duration of 3 h. We present the results for several PAHs in Fig. 17. We were able to derive the destruction rate by monitoring the aromatic C=C stretching vibrations of PAHs around

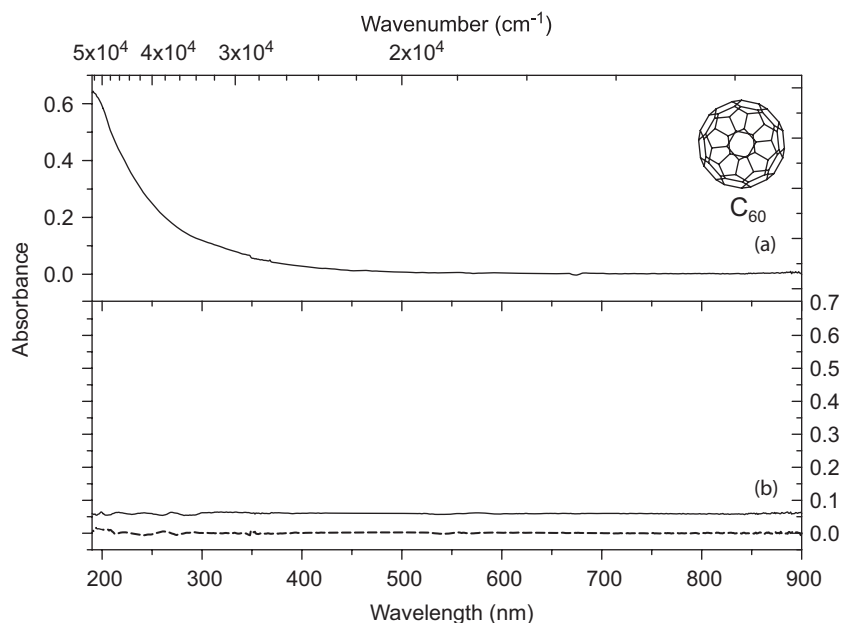


Fig. 16. Top graph shows the UV/Vis spectrum of a C<sub>60</sub> film (~100 nm) deposited on a MgF<sub>2</sub> disk. See the figure caption of Fig. 8 for an explanation of the graph contents.

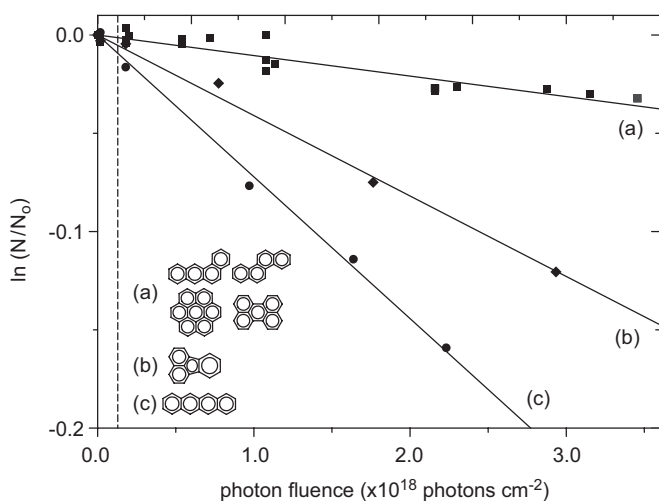


Fig. 17. BIOPAN sample cells containing thin PAH films were exposed under vacuum in a laboratory setup using a hydrogen discharge lamp (duration of 3 h). The natural logarithm of the normalized integrated absorbance  $\ln(N/N_0)$  is plotted against photon fluence. The slope of the linear fit through  $\ln(N/N_0)$  represents the destruction rate. The photo-destruction of selected molecules is displayed. Trace (a) shows a high photostability for the PAHs: 1,2-benzanthracene, chrysene, coronene and perylene under the specific experimental conditions. We can observe that fluoranthene and 2,3-benzanthracene: traces (b) and (c) show photo-destruction rates that are some 4 and 7 times higher than for the other larger PAHs. The BIOPAN equivalent fluence for 58.8 h and 7.4 eV photons (vertical dashed line) correspond to 0.12 ( $10^{18}$  photons  $\text{cm}^{-2}$ ) which is consistent with the observed degradation rate smaller than 1%.

$1600\text{ cm}^{-1}$  by IR spectroscopy. The decreasing integrated intensity of this band permits to measure the residual fraction  $N/N_0$  of the PAH compound as a function of photon fluence. The C = C stretching vibration can be well

measured as isolated band and the decrease of this band can be directly related to the disruption of aromatic rings (the carbon skeleton). The C–H stretching and bending modes would only give a measurement of dehydrogenation of the individual PAHs.

Based on these results we observe that most PAHs have small destruction rates upon UV exposure of 3 h in these laboratory experiments. However, we can observe that fluoranthene and 2,3-benzanthracene (traces (b) and (c) in Fig. 17, respectively) show photodestruction rates that are some 4 and 7 times higher than the other larger PAHs. Note that since the emission spectrum of this UV lamp does not resemble the solar UV emission field we only compare these laboratory results with the BIOPAN results with caution. For the bands 115–125, 150–170, 170–195 nm, the UV lamp flux is respectively 1, 17.5, 14 (in  $10^{13}$  photons  $\text{cm}^{-2}\text{ s}^{-1}$ ), while the solar flux is, respectively 6, 6 and 55 (in  $10^{11}$  photons  $\text{cm}^{-2}\text{ s}^{-1}$ ). In these respective wavelength ranges the fluence of the lamp for 3 h exposures is 0.11, 1.9, 1.5 ( $10^{18}$  photons  $\text{cm}^{-2}$ ), while the BIOPAN solar fluence for 58.8 h is 0.13, 0.13, 1.2 ( $10^{18}$  photons  $\text{cm}^{-2}$ ). If we assume an average photon energy of 7.4 eV for our laboratory UV lamp (Cottin et al., 2003) we observe that the same energy fluence that was observed during the BIOPAN flight (i.e.  $1.367\text{ [kJ m}^{-2}\text{)]}$  relates to a photon fluence of  $1.2 \times 10^{17}$  photons  $\text{cm}^{-2}$  in our laboratory. However, if we assume an effective photon cut off energy of 6.3 eV for 195 nm then the BIOPAN exposure of 58.8 h would relate to a fluence of 10 times higher. The measured photodestruction rate in the BIOPAN experiment below 1% is consistent with the threshold for photo-destruction energy higher than 7 eV, even if there are 10 times more solar photons at 6 eV.

## 5. Conclusions

PAHs play an important role in the carbon chemistry and the physical and chemical evolution of the ISM. They can be present in different charge and hydrogenation states and be dissociated by energetic processes. The formation of radicals and ions adds an additional important dimension to the chemistry of carbon-based molecules in the ISM. Moreover the physical conditions in the ISM could lead to a selection mechanism that favors specific PAHs. To gain a better and more accurate understanding of the distribution of PAHs and PAH-like species in space it is important to test the stability of PAHs in situ in a space environment. We exposed 17 PAH samples to the solar UV and visible emission spectrum in LEO. The ORGANICS experiment on BIOPAN V fulfilled the goal as precursor for a long-term exposure experiment on the ISS. The sample deposition, handling and pre- and post-flight analysis were sufficient to characterize the PAH films before and after exposure to NEO UV flux. AFM images of the samples revealed crystal structures covering the surface rather than homogeneous layers. We may need to improve the film quality for these PAHs or choose alternative PAH samples for the longer exposure experiment on ISS. No substantial changes were found in the column densities of the PAH films measured before and after exposure to the LEO environment, confirming the photostability of PAHs in space environments. Moreover, we found no evidence for dehydrogenation from monitoring the evolution of the C–H stretching and/or bending modes in the IR spectra of samples measured before and after exposure to the LEO environment. The gas-phase ionization potentials for the PAHs selected in these exposure experiments are in the order of 6–7 eV. The choice of materials in the sample cells assured transmission of photons with energies up to 10.2 eV so we expect that ions can be formed. However, there was no evidence of any ion chemistry in the exposed PAH films for the observed flux levels and exposure times. Based on the differences observed between the UV-exposed films and unexposed control samples we could derive upper limits for the destruction of some PAHs. These values are less than 1% for most PAHs. These small differences in absorption between the samples are within the experimental uncertainties (i.e., error bars). Therefore, we conclude that we found no evidence for photodestruction of the PAH and fullerene C<sub>60</sub> samples that were exposed for nearly 16 days to LEO in this flight experiment.

We have compared the space exposure results with laboratory simulations in which we exposed a number of the PAH samples to the UV flux of a hydrogen discharge lamp. The hydrogen flow lamp emits photons between 150 and 195 nm at an average flux of  $3.2 \times 10^{14}$  photons cm<sup>-2</sup> s<sup>-1</sup> and average photon energies of 7.4 eV (see Cottin et al., 2003 for lamp spectrum and flux details). The total absorbed fluence that was observed during the BIOPAN flight relates to an average laboratory lamp

fluence of  $1.2 \times 10^{17}$  photons cm<sup>-2</sup> for an effective energy of 7.4 eV. We note from Fig. 17 that indeed no photodestruction is expected for those fluences confirming earlier laboratory experiments (for a review see Salama, 1999). What will determine photolysis and ionization efficiencies are the photons above 7 eV.

We conclude that PAH molecules are indeed stable against UV irradiation. The selected PAHs that were exposed to the solar UV field easily survived the conditions of LEO for the duration of the BIOPAN V flight. For the low-energy dose that was absorbed by the PAH films during the BIOPAN flight we find no conclusive evidence for photo-destruction. However, we do expect to find photo-destruction for the long irradiation times expected for the EXPOSE experiment on ISS (fluences of up to  $10^{20}$  photons cm<sup>-2</sup> are expected between 120 and 200 nm).

The ORGANICS experiment on BIOPAN V is a precursor for a longer-duration exposure experiment on the EXPOSE experiment platform on ISS. The time-integrated irradiance during the BIOPAN V flight was small compared to the time integrated irradiance of PAHs in the ISM. PAHs in the ISM experience a photon flux of  $10^8$  photons cm<sup>-2</sup> s<sup>-1</sup> integrated from 90 to 250 nm (Mathis et al., 1983). The solar UV emission spectrum is very different from the interstellar radiation field (Draine, 1978; Roberge et al., 1991) with a monochromatic flux  $10^5$  higher at 180 nm (at 7 eV) and more than  $10^6$  higher above 200 nm (below 6 eV). For processes relevant to the energy range at 7 eV, the space exposure experiments such as BIOPAN (380 h, with 15 % effective solar pointing) can simulate 600 years diffuse interstellar radiation field, and ISS/Expose (3 yr, 15% solar pointing) can simulate 50,000 years in the diffuse medium.

## Acknowledgments

The authors wish to thank Rene Demets and Pietro Baglioni for their support during mission planning, Christiaan Pen for his help in the design and manufacturing of the experiment hardware and Sasha Kolobkov for his help with the AFM analysis. We also thank Werner Schmitt for discussion. We thank the R3D experiment team for providing radiation and temperature flight data. The ORGANICS on BIOPAN V experiment was funded under SRON program MG-049 and NWO-VI 016.023.003.

## References

- Allain, T., Leach, S., Sedlmayr, E., 1996a. Photodestruction of PAHs in the interstellar medium. I. Photodissociation rates for the loss of an acetylenic group. *Astron. Astrophys.* 305, 602–615.
- Allain, T., Leach, S., Sedlmayr, E., 1996b. Photodestruction of PAHs in the interstellar medium. II. Influence of the states of ionization and hydrogenation. *Astron. Astrophys.* 305, 616–630.
- Allamandola, L.J., Hudgins, D.M., Sandford, S.A., 1999. Modeling the unidentified infrared emission with combinations of polycyclic aromatic hydrocarbons. *Astrophys. J.* 511, 115–119.

- Becker, L., Bunch, T.E., 1997. Fullerenes, fulleranes and PAHs in the Allende meteorite. *Meteoritics* 32, 479–487.
- Cataldo, F., 2004. From elemental carbon to complex macromolecular networks in space. In: Ehrenfreund, et al. (Eds.), *Astrobiology: Future Perspectives*. Astrophysics and Space Science Library 305, Kluwer Academic Publishers, Dordrecht, pp. 97–126.
- Cottin, H., Moore, M.H., Bénilan, Y., 2003. Photodestruction of relevant interstellar molecules in ice mixtures. *Astron. Astrophys.* 590, 874–881.
- Dartois, E., Marco, O., Muñoz-Caro, G.M., Brooks, K., Deboffle, D., d'Hendecourt, L., 2004. Organic matter in Seyfert 2 nuclei: Comparison with our Galactic center lines of sight. *Astron. Astrophys.* 423, 549–558.
- Demets, R., Schulte, W., Baglioni, P., 2005. The past, present and future of BIOPAN. *Adv. Space Res.* 36/2, 311–316.
- Draine, B., 1978. Photoelectric heating of interstellar gas. *Astrophys. J. Suppl.* 36, 595–619.
- Ehrenfreund, P., Charnley, S.B., 2000. Organic molecules in the ISM, comets and meteorite: A voyage from dark clouds to the early Earth. *Ann. Rev. Astron. Astrophys.* 38, 427–483.
- Foing, B.H., Ehrenfreund, P., 1994. Detection of two interstellar absorption bands coincident with spectral features of  $C_{60}^+$ . *Nature* 369, 296–298.
- Foing, B.H., Ehrenfreund, P., 1997. New evidences for interstellar  $C_{60}^+$ . *Astron. Astrophys.* 317, 59–62.
- Frenklach, M., Feigelson, E.D., 1989. Formation of polycyclic aromatic hydrocarbons in circumstellar envelopes. *Astrophys. J.* 341, 372–384.
- Henning, T., Salama, F., 1998. Carbon in the Universe. *Science* 282, 2204–2210.
- Henning, Th., Jäger, C., Mutschke, H., 2004. Laboratory studies of carbonaceous dust analogs astrophysics of dust. In: Witt, A.N., Clayton, G.C., Draine, B.T. (Eds.), *The Astrophysics of Dust*. ASP Conference Series 309, San Francisco, pp. 603–628.
- Herbig, G.H., 1995. The Diffuse Interstellar Bands. *Annu. Rev. Astron. Astrophys.* 33, 19–74.
- Krätschmer, W., Lamb, L., Fostiropoulos, K., Huffman, 1990. Solid C60: a new form of Carbon. *Nature* 347, 354–358.
- Kroto, H.W., Heath, J.R., O'Brien, S.C., Curl, R.F., Smalley, R.E., 1985. C60: Buckminsterfullerene. *Nature* 318, 162–163.
- Le Page, V., Snow, T.P., Bierbaum, V.M., 2001. Hydrogenation and charge states of PAHs in diffuse clouds. I. Development of a model. *Astrophys. J. Suppl. Series* 132, 233–251.
- Mathis, J.S., Mezger, P.G., Panagia, N., 1983. Interstellar radiation field and dust temperatures in the diffuse interstellar matter and in giant molecular clouds. *Astron. Astrophys.* 128, 212–229.
- Mennella, V., Colangeli, L., Bussoletti, E., Palumbo, P., Rotundi, A., 1998. A new approach to the puzzle of the ultraviolet interstellar extinction bump. *Astrophys. J.* 507, 177–180.
- Pascoli, G., Polleux, A., 2000. Condensation and growth of hydrogenated carbon clusters in carbon-rich stars. *Astron. Astrophys.* 359, 799–810.
- Peeters, Z., Botta, O., Charnley, S.B., Ruitenkamp, R., Ehrenfreund, P., 2003. The astrobiology of nucleobases. *Astrophys. J.* 593 (2), L129–L132.
- Pendleton, Y., Allamandola, L., 2002. The organic refractory material in the diffuse interstellar medium: mid-infrared spectroscopic constraints. *Astrophys. J. Suppl.* 138, 75–98.
- Roberge, W.G., Jones, D., Lepp, S., Dalgarno, A., 1991. Interstellar photodissociation and photoionization rates. *Astrophys. J. Suppl.*, 287–297.
- Ruitenkamp, R., Peeters, Z., Moore, M., Hudson, R., Ehrenfreund, P., 2005a. A quantitative study of proton irradiation and UV photolysis of benzene in interstellar environments. *Astron. Astrophys.* 440, 391–402.
- Ruitenkamp, R., Cox, N.L.J., Spaans, M., Kaper, L., Foing, B.H., Salama, F., Ehrenfreund, P., 2005b. PAH charge state distribution and DIB carriers: Implications from the line of sight toward HD 147889. *Astron. Astrophys.* 431, 515–529.
- Salama, F., 1999. Polycyclic aromatic hydrocarbons in the interstellar medium: a review. In: d'Hendecourt, L., Joblin, C., Jones, A. (Eds.), *Solid Interstellar Matter: The ISO Revolution*. EDP Sciences, Springer, Les Ullis, pp. 65–89.
- Salama, F., Bakes, E.L.O., Allamandola, L.J., Tielens, A.G.G.M., 1996. Assessment of the polycyclic aromatic hydrocarbon—diffuse interstellar band proposal. *Astron. Astrophys.* 458, 621–636.
- Tielens, A.G.G.M., Hony, S., van Kerckhoven, C. and Peeters, E., 1999. Interstellar and circumstellar PAHs. In: *The Universe as seen by ISO*, ESA SP 427, pp. 579–588.
- Vuong, M.H., Foing, B.H., 2000. Dehydrogenation of polycyclic aromatic hydrocarbons in the diffuse interstellar medium. *Astron. Astrophys.* 363, L5–L8.
- Yan, L., Chary, R., Armus, L., Teplitz, H., Helou, G., Frayer, D., Fadda, D., Surace, J., Choi, P., 2005. Spitzer detection of polycyclic aromatic hydrocarbon and silicate dust features in the mid-infrared spectra of  $z \sim 2$  ultraluminous infrared galaxies. *Astrophys. J.* 628, 604–610.